Article ID: 1000-7032(2013)02-0184-08

Optical Analysis and Optimization of Lossless and Lossy Distributed Bragg Reflector Using Transfer Matrix Method

WANG Yun-hua, BO Bao-xue *

(*State Key Laboratory of High Power Semiconductor Lasers, Changchun University of Science and Technology, Changchun* 130022, *China*)

* *Corresponding Author, E-mail: bbx*2001@163. *com*

Abstract: The optical analysis of the lossless and lossy distributed Bragg reflector (DBR) structure using the transfer matrix method was reported. For DBR structures with different configurations of HL, HLH, LH and LHL, the optical field distributions were gained from the simulation. The theoretical analysis showed that the level of optical field amplitude within HL and HLH structure was much lower than other structures. For the extinction coefficient of 0.01, the energy absorption in HL and HLH DBR structures was only 10% of the one within LH and LHL structures. Due to the optical absorption, the reflectivity at the central wavelength of HL and HLH DBR structures decreased by 3.6%, comparing with 29.2% for LH and LHL structures. Thus, the reflectivity of DBR could be increased if the high index layer was used as the first layer, and the optical absorption could be decreased by this method. At last, the lossy DBR consisted of $Al_{0.12}Ga_{0.88}As/Al_{0.9}Ga_{0.1}As$ was grown and its reflectivity was measured.

Key words: transfer matrix method; distributed Bragg reflector; optical field distribution; reflectivity spectrum
CLC number: O472.3　　**Document code**: A　　**DOI**: 10.3788/fgxb20133402.0184

无损耗型及损耗型分布布拉格反射镜光学特性的传输矩阵理论分析及优化

王云华，薄报学 *

（长春理工大学 高功率半导体激光国家重点实验室，吉林 长春　130022）

摘要：利用传输矩阵理论对无光学损耗和有光学损耗的分布布拉格反射镜(Distributed Bragg reflector,DBR)分别进行了结构分析与优化。在光场正入射条件下,对具有 HL、HLH、LH 及 LHL 结构的 DBR 内部光场分布情况进行了模拟分析和实验验证。结果表明:光场正入射到 DBR 后,在 HL 及 HLH 型 DBR 结构内部的光场分布最弱。当组成 DBR 的材料层消光系数为 0.01 时,HL 及 HLH 型 DBR 内部产生的能流密度吸收量最小,为其他结构的 10% 左右,材料吸收引起的中心波长反射率降低仅为 3.6%;而 LH 及 LHL 型 DBR 结构由于材料吸收而导致反射率降低 29.2%。因此,采用高折射率材料层作为 DBR 结构的第一层有利于提高 DBR 反射率,降低光学吸收。最后,通过 MOCVD 外延生长了具有 HL 结构的吸收型 $Al_{0.12}Ga_{0.88}As/Al_{0.9}Ga_{0.1}As$ DBR 结构,并对其反射特性进行了测试。

关　键　词：传输矩阵法；分布布拉格反射器；光场分布；反射光谱

收稿日期：2012-11-20；**修订日期**：2012-12-08
基金项目：国家自然科学基金(61177019,61176048)资助项目
作者简介：王云华(1984 -)，女，吉林公主岭人，主要从事半导体薄膜生长的研究。
E-mail：qqgirlwyh@163. com

1 Introduction

Multilayer structure of alternating quarter-wave layers of high and low refractive index known as distributed Bragg reflector (DBR) is usually made of dielectric or semiconductor material. DBRs possessing good reflecting characteristics have been widely applied in semiconductor optoelectronic devices such as vertical cavity surface emitting lasers (VCSELs)[1-2], resonant cavity light emitting diodes (RCLEDs)[3] and resonant cavity enhanced photodetectors (RCEPDs)[4]. DBR with high reflectance and low optical absorption is needed to provide an efficient operation in these devices[5]. High reflectance of DBR mirror is normally attained at great number of layers, while absorption loss in the layers of multilayer mirrors diminishes their reflectance[6-7]. Thus it is important to reveal optimal structure of the DBR *via* correcting computer modeling before costly fabrication process.

Mathematical methods such as the coupled mode theory (CMT)[8], the finite difference time domain method (FDTDM)[9], and transfer matrix method (TMM)[10-11] *etc* have been applied in practical design of DBR in different devices in the past few decades. Influences of low absorption loss in layers of DBR on its reflective properties had been analyzed and DBR with high reflectance and low loss was got by using a high refractive index as the first layer[12]. This conclusion was explained by the different penetration depth of light in the structure. H. V. Baghdasaryan[13] investigated the relation between lossy characteristics in the DBR and optical fields by the method of single expression. However, the physical mechanism of above conclusion would be more clearly if the optical field distribution within DBRs was analyzed.

In this paper, the optical field distribution was deduced by transfer matrix method, which is well known for its peculiarities of high accuracy and easy understanding. The physical mechanism of loss impact on DBR reflectance was clarified through the detailed analysis of optical field and power flow density distribution within different DBR structures. Applications of different DBRs for corresponding semiconductor optoelectronic devices were also discussed.

2 Modeling and Experiment

Detailed description of the TMM had been presented in Ref. 10 and 11. And the main principle of TMM was shown in Fig. 1.

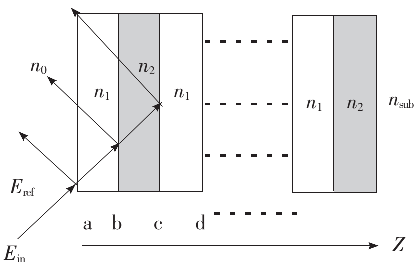

Fig. 1 DBR structure consisting of alternating quarter-wave layers for the analysis using transfer matrix method

As shown in Fig. 1, the DBR structure consisted of alternating quarter wave layers. Optical thicknesses of every layer was a quarter of wavelength, that is to say, $\lambda = 4n_1 d_1 = 4n_2 d_2$, and λ was the central wavelength, n and d were the refractive index and thickness of materials. The normal incidence of linearly polarized plane electromagnetic wave on the DBR structure was considered.

When the electromagnetic wave came from interface (a) to (b), the following transfer matrix could be obtained:

$$\begin{bmatrix} B \\ C \end{bmatrix} = \begin{bmatrix} \cos\delta_1 & \mathrm{i}\sin\delta_1/n_1 \\ \mathrm{i}n_1\sin\delta_1 & \cos\delta_1 \end{bmatrix}\begin{bmatrix} 1 \\ n_2 \end{bmatrix}, \qquad (1)$$

Here the phase changes $\delta_1 = \frac{2\pi N_1}{\lambda}\cos\theta_1 \cdot d_1$ for s waves and $\delta_1 = \frac{2\pi N_1}{\lambda\cos\theta_1} \cdot d_1$ for p waves. $N_1 = n_1 - \mathrm{i}k_1$ was the refractive index of the first layer, and k_1 was known as the extinction coefficient. We defined relations $Y = C/B$. And the intensity coefficients of reflection and transmission could be expressed as:

$$R = \left(\frac{n_0 - Y}{n_0 + Y}\right) \cdot \left(\frac{n_0 - Y}{n_0 + Y}\right)^*, \qquad (2)$$

$$T = \frac{4n_0 n_{sub}}{(n_0 B + C)(n_0 B + C)^*}. \qquad (3)$$

The sign of n_0 and n_{sub} indicated the refractive index of the medium from which the optical wave came and the medium to which the optical wave went out. For the structure consisting of m layers, the transfer matrix could be expressed in the form of multiplication:

$$\begin{bmatrix} B \\ C \end{bmatrix} = \prod_{j=1}^{m} \begin{bmatrix} \cos\delta_j & \mathrm{i}\sin\delta_j / n_j \\ \mathrm{i} n_j \sin\delta_j & \cos\delta_j \end{bmatrix} \begin{bmatrix} 1 \\ n_{\mathrm{sub}} \end{bmatrix}. \quad (4)$$

By setting the amplitude of optical field in the incident medium at fixed amplitude $|E_a| = 1$, the optical field distribution within the DBR could be deduced. The power loss of the wave absorbed in any 1D structure was proportional to the optical field component's intensity $|E_z|^2$, the frequency ω corresponding to the incident wavelength, the permittivity of air ε_0, the imaginary part of the permittivity ε'' and the length of the structure L. The power loss could be described[14]:

$$P_{\mathrm{loss}} = \omega\varepsilon_0 \int_0^L \varepsilon''(z) \, |E_z|^2 \mathrm{d}z, \quad (5)$$

Where ε'' could be related to the extinction coefficient k from equations:

$$\varepsilon = \varepsilon' + \mathrm{i}\varepsilon'' = N^2 = (n + \mathrm{i}k)^2. \quad (6)$$

At last, the sample of $Al_{0.12}Ga_{0.88}As/Al_{0.9}Ga_{0.1}As$ distributed Bragg reflector (DBR) mirrors was grown on GaAs substrate without any growth interruptions or purging sequences at the interfaces. The designed central wavelength of DBR structure was 980 nm. Scanning electron microscope (SEM) and reflectivity spectrum tests were carried out to confirm the design principle.

3 Results and Discussion

3.1 Lossless DBRs at Central Wavelength

DBR structure with central wavelength at λ = 800 nm had the condition $\lambda/4 = n_H d_H = n_L d_L$. Here, $n_H = 3.5659$ and $n_L = 3.0854$ were chosen as the high and low refractive index of the alternating layers, d_H and d_L were the layers' thickness. Lossless DBRs meant that the extinction coefficient of material equaled zero ($k = 0$), thus none optical loss existed in this structure. In Fig. 2, four types of DBR structures with even and odd number of layers were considered. The even number of layers in Fig. 2(a) and Fig. 2(c) consisted of 15 pairs of high and low index layers, while the Fig. 2(a) started

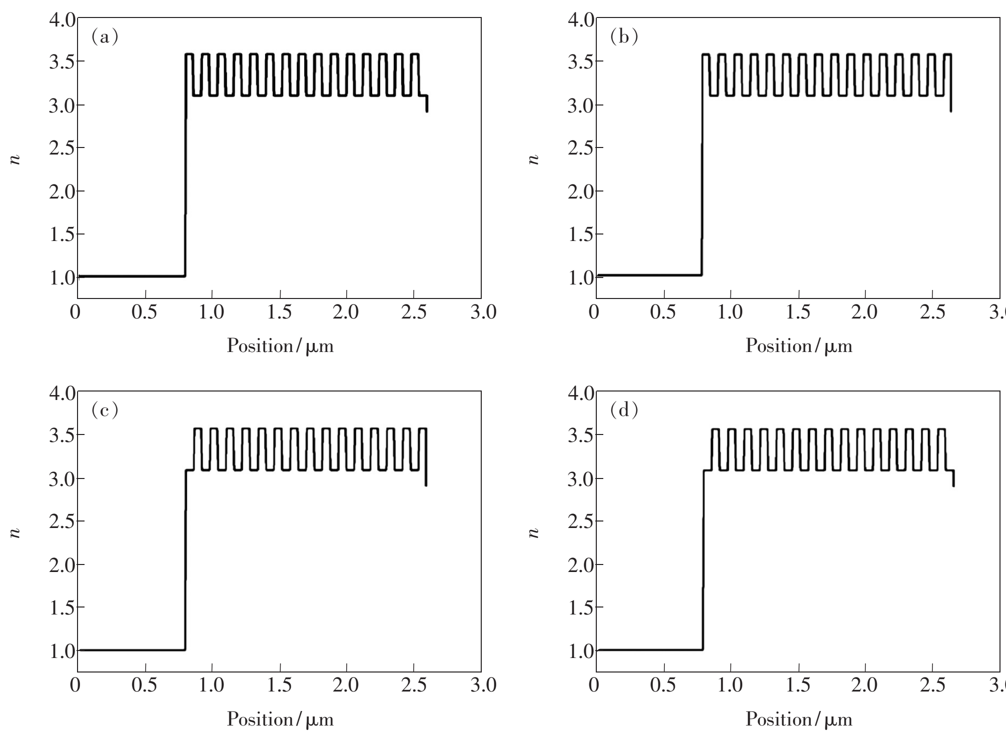

Fig. 2 Refractive index profiles of different DBR structures composed of bilayers: Even number of layers starting by n_H (a) and odd number of layers starting and ending by n_H (b); Even number of layers starting by n_L (c) and odd number of layers starting and ending by n_L (d).

from the layer of high refractive index, and the Fig. 2 (c) started from the low refractive index. Adding the first layer of Fig. 2(a) and Fig. 2(c) to the end, we got the structure of Fig. 2(b) and Fig. 2 (d). These four types of DBR structure were called having the form of HL, HLH, LH, and LHL, respectively. In these structures, the refractive index of incident medium and output medium were 1 and 2.9, respectively.

In Fig. 3, the distributions of optical field amplitude of four types of DBR structures (presented in Fig. 2) were shown at fixed amplitude of the optical field in the incident medium (E_{inc} = 1 a. u.). Of course, the value of amplitude could be taken as arbitrary one.

For each DBR structure, the standing wave pattern was formed as a result of superposition of incident and reflected waves, as shown in Fig. 3. But the distribution of optical field within DBR was different from each other. In structures of HL and HLH, it started from the layer of high refractive index, the left boundary of the first layer was located at the node of optical field amplitude, while in structures LH and LHL, this boundary was located at the antinode of the field amplitude. As a result, in these structures, the high intensity incident field at the left boundary of the first layer could cause damage of a mirror in structures LH and LHL. For high power diode lasers using DBR as the reflective film of cavity, we should consider this.

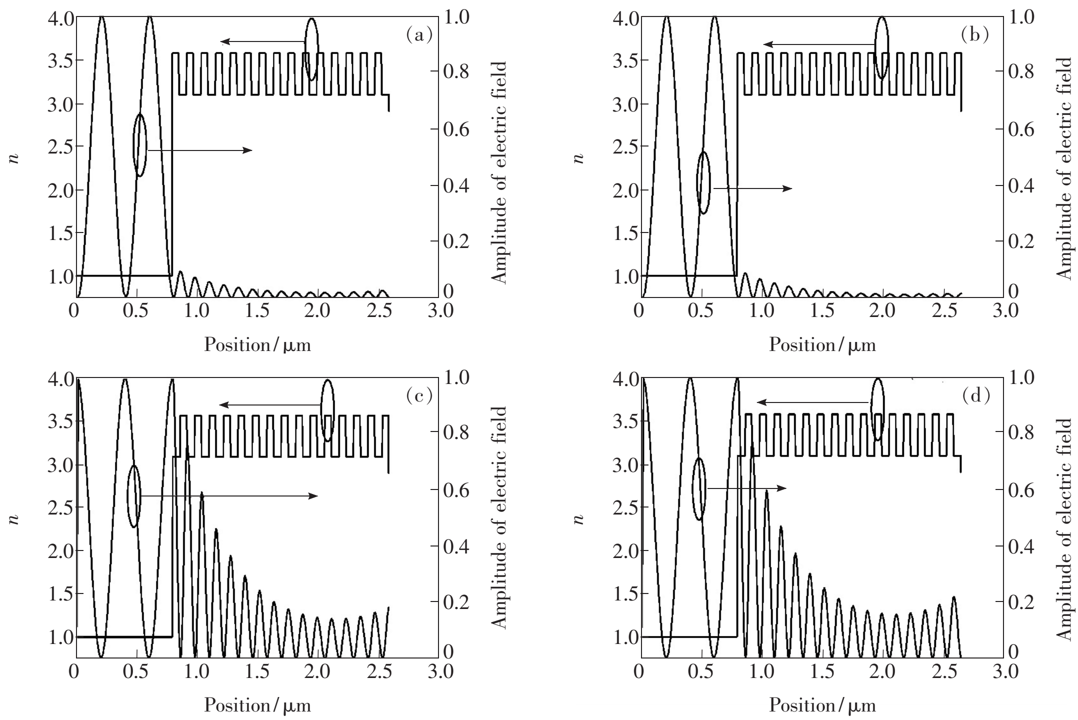

Fig. 3 Optical field amplitude distribution in DBRs structures of (a) ~ (d), corresponding to structures of HL, HLH, LH and LHL. The amplitude of optical field in the incident medium is fixed: E_{inc} = 1.

In all considered structures, amplitude of optical field decayed starting from the interface between the incident medium and the first layer towards the end of the structure, but non-monotonicity for all the structures was observed (even for Fig. 3(a) and Fig. 3(b) if they were enlarged). This was different from the result of Ref. 13 in which only the characteristic of non-monotonicity was observed in structures of HL and LHL, and this phenomenon was not explained either. Optical interference would be the main reason for the optical characteristics of DBR because of the coherence of the DBR layers with the same optical thickness between two adjacent interfaces. Optical field would have a constructive interference if the difference of optical path of two optical waves was the integral multiple of the wavelength, while the destructive interference would appear when the difference of optical path was the odd times of the half wavelength. The constructive and destructive interference influenced the distribution of optical field within the DBR simultaneously. On the illuminated side of the structures (in the incident medium), the interface realized the maximum constructive interference. When the position moved towards the end of the structure, the reflectance of the right part would decrease gradually because of the less number of layers of DBR. The constructive interference would also become weaker, and the destructive interference played more important role in influencing the optical field. For these reasons, the amplitude of optical wave would decrease with the increasing position. But at the last few layers, the destructive interference became weaker due to the smaller number of layers which could generate the destructive interference, thus, the amplitude of optical wave increased at the end of these structures.

The envelopes of optical field amplitude in Fig. 3(a) and 3(b) within the DBR were obviously lower than that in Fig. 3(c) and 3(d). Thus, the value of first layer's refractive index determined the value of optical field within the structure. With the layer of lower index as the first layer, optical field transmitted deeper than the structure with the first layer of high refractive index. This conclusion corresponded to the analysis from Ref. 12 and 15 in which the transmitting depth was calculated for different structures.

3.2 Optical Characteristics of Lossy DBRs

DBR structures used in semiconductor devices always consisted of semiconductor materials, in which the optical absorption existed. It was thus favorable to analyze the influence of loss on optical characteristics of different types of DBR structures. Some preliminary results were already got using MSE method in Ref. 13. Here the TMM method was used to carry out the analysis of the optical absorption influence on DBR distribution of optical field and spectrum of reflectance. Analysis started from the assumption that the extinction coefficient k equaled 0.01 for materials of both high refractive index and low refractive index.

To make a deeper investigation of the loss influence on reflective property of DBRs, it was useful to present distributions of the optical field amplitude and the absorption of power flow density P_{loss} from Eq. 5 in the considered lossy DBR structures. Corresponding distributions of optical field at $k = 0.01$

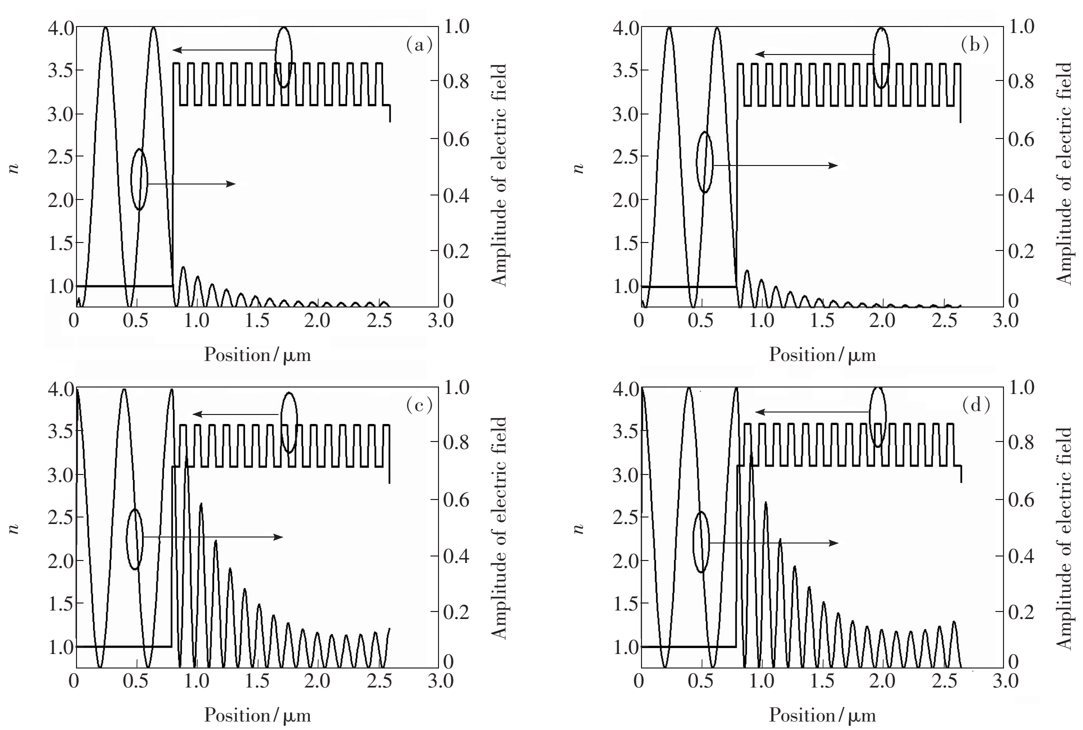

Fig. 4 Optical field amplitude distribution in lossy DBRs structures of (a) ~ (d). The amplitude of optical field in the incident medium is fixed: $E_{inc} = 1$, and the extinction coefficient $k = 0.01$.

were presented in Fig. 4. Amplitude of optical field in Fig. 4 was a little lower than in Fig. 3 caused by the optical absorption. However, the non-monotonic characteristics of optical field for all the structures still existed. And the locations of the node and anti-node of optical field amplitude in Fig. 4 were the same as that in Fig. 3. Thus the optical absorption had no influence on the distribution of optical field, but it had much influence on the distribution of optical intensity.

The optical loss characterized by $\frac{P}{\omega\varepsilon_0}$ (equals $\int_0^L \varepsilon''(z)\,|E_z|^2\,\mathrm{d}z$ from Eq. 5) was shown in Fig. 5. In all structures, stepwise increase of optical loss was observed, which was caused by the oscillating character of optical field amplitude along the structures. It was clearly shown that the structures of LH and LHL had a more rapid increasing of optical loss than the structures of HL and HLH. The total optical loss within LH and LHL DBR was about 10 times than that in HL and HLH DBR structure. This could be explained by the distribution of optical field amplitude in different structures. In the structure of LH and LHL, the envelopes of optical field amplitude were relatively high, thus, it induced high optical loss. Structures of HL and HLH would suffer lower loss because of the lower envelopes of optical amplitude within DBRs.

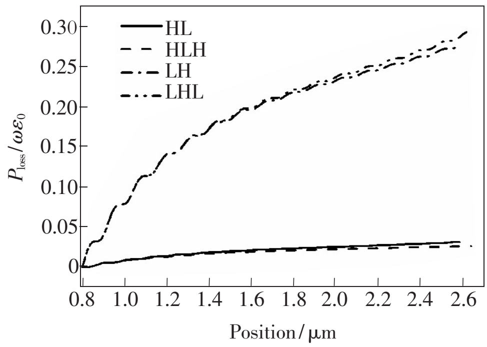

Fig. 5　Absorption of energy flow density within different structures

The spectral characteristics of structures in Fig. 2 with and without optical loss were calculated by the TMM and presented in Fig. 6. The presence of loss brought the general decrease in reflectance within the wavelength band. In the structures with higher envelope of internal optical field amplitude, the influence of loss was stronger. For structures of LH and LHL, the presence of loss brought a relatively

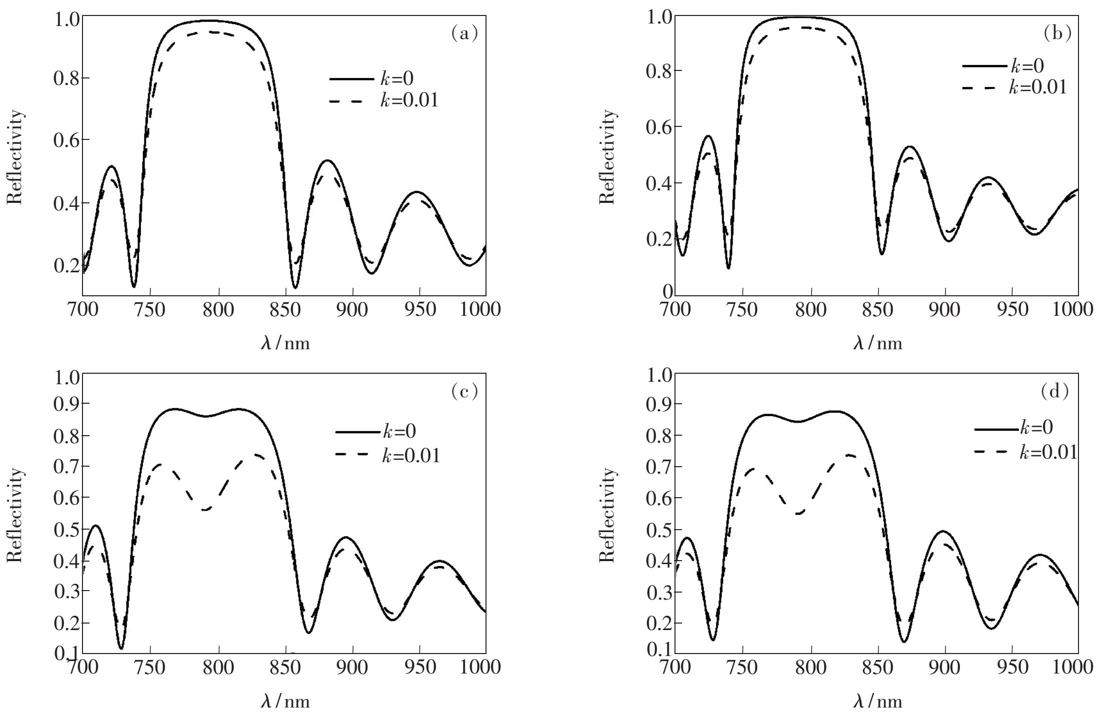

Fig. 6　Reflectivity spectra with and without loss in the layers of four different structures corresponding to HL (a), HLH (b), LH (c), and LHL (d).

high decrease in the reflectance within the main wavelength band, and the reflectance decreased by 29.2% at the central wavelength (Fig. 6(c) and 6(d)). For structures of HL and HLH, the decrease in the reflectance was not so high (Fig. 6(a) and 6(b)), and the reflectance decreased only by 3.6% at the central wavelength. Large decrease of the reflectance at the central wavelength of structures LH and LHL was explained by strong impact of loss on central wavelength for these structures.

3.3 Growth and Measurements of Lossy DBR Structure

The DBR structure of 23 pairs of $Al_{0.12}Ga_{0.88}As$/$Al_{0.9}Ga_{0.1}As$ layers was grown by MOCVD, and the

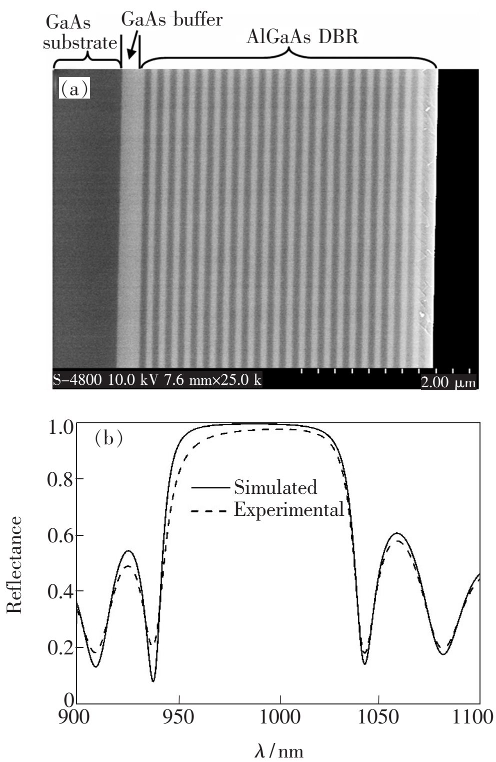

Fig. 7 Scanning electron microscope test result (a) and reflectivity spectra (b) of grown DBR structure, central wavelength was 980 nm as expected.

central wavelength was designed at 980 nm. The structure of HL (Fig. 2(a)) was employed to gain good characteristics. Scanning electron microscope (SEM) test was carried out after the growth of DBR structure, with the result shown in Fig. 7(a). Good periodicity of alternating $Al_{0.12}Ga_{0.88}As$/$Al_{0.9}Ga_{0.1}As$ layers was observed. Reflectivity spectrum was gained employing the device of lambda 1050 UV/Vis/NIR Spectrophotometer, as shown in Fig. 7(b). The expected reflectivity spectrum was also simulated using TMM. The maximum and local maximum reflectances of measured result were consistent, but it was smaller than the simulated one, which was caused by the optical absorption in the grown structure. The central wavelength and bandwidth of reflectivity spectrum were also consistent, and the flat reflective spectrum within the bandwidth was observed, just as the theoretical analysis in Fig. 6(a). Thus the experimental result proved the reliability of DBR design theory we proposed.

4 Conclusion

In this paper, the optical characteristics of lossless and lossy DBRs were analyzed in detail by the transfer matrix method with plane electromagnetic wave normal incidence. The optical field distributions within different DBR structures were obtained and a detailed analysis to the optical field characteristics was carried out. Preliminary analysis showed that DBRs starting and ending by a quarter wavelength layer of high refractive index provided the highest reflectance and lowest optical loss. The lossy DBR structure was grown and measured. Measured reflectivity spectrum showed that the design theory we proposed was reliable in designing the DBR structures.

References:

[1] Iga K. Surface-emitting laser—Its birth and generation of new optoelectronics field [J]. *IEEE J. Sel. Top. Quant.*, 2000, 6(6):1201-1215.

[2] Li H, Iga K. *Vertical-cavity Surface—Emitting Laser Devices* [M]. Berlin Heidelberg: Springer, 2002:56-59.

[3] Wang Y H, Cho A Y, Tu L W, *et al*. Resonant cavity light-emitting diode [J]. *Appl. Phys. Lett.*, 1992, 60(8):921-923.

[4] El-Batawy Y M, Deen M J. Resonant cavity enhanced photodetectors (RCE-PDs): Structure, material, analysis and optimization [J]. *SPIE*, 2003, 4999:363-378.

[5] Passaro V M N, Magno F, de Leonardis F. Optimization of Bragg reflectors in AlGaAs/GaAs VCSELs [J]. *Laser Phys. Lett.*, 2005, 2(5):239-246.

[6] Murtaza S S, Anselm K A, Srinivasan A, *et al*. High-reflectivity Bragg mirrors for optoelectronic applications [J]. *IEEE J. Quantum Elect.*, 1995, 31(10):1819-1825.

[7] Asplund C, Mogg S, Plaine G, *et al*. Doping-induced losses in AlAs/GaAs distributed Bragg reflectors [J]. *J. Appl. Phys.*, 2001, 90(2):794-800.

[8] Matuschek N, Kartner F X, Keller U, *et al*. Exact coupled-mode theories for multilayer interference coatings with arbitrary strong index modulations [J]. *IEEE J. Quantum Elect.*, 1997, 33(3):295-302.

[9] Taflove A, Hagness S C. *Computational Electrodynamics: The Finite Difference Time Domain Method* [M]. Boston: Artech House, 2000.

[10] Born M, Wolf E. *Principles of Optics* [M]. 5th ed. Oxford: Pregamon Press, 1975:190-191.

[11] Macleod H A. *Thin-film Optical Filters* [M]. 3rd ed. Bristol, Philadelphia: Institute of Physics Pub, 2001.

[12] Babic D I, Corzine S W. Analytic expressions for the reflection delay, penetration depth, and absorptance of quarter-wave dielectric mirrors [J]. *IEEE J. Quantum Elect.*, 1992, 28(2):514-524.

[13] Baghdasaryan H V, Knyazyan T M, Baghdasaryan T H, *et al*. Absorption loss influence on optical characteristics of multilayer distributed Bragg reflector: Wavelength-scale analysis by the method of single expression [J]. *Opto-Electron. Rev.*, 2010, 18(4):438-445.

[14] Landau L D, Lifshitz E M, Pitaevskii L P. *Electrodynamics of Continuous Media* [M]. 2nd ed. Oxford & New York: Butterworth-Heinemann Press, 1984.

[15] Kavokin A V, Kaliteevski M A. Light-absorption effect on Bragg interference in multilayer semiconductor heterostructures [J]. *J. Appl. Phys.*, 1996, 79(2):595-598.